

Received April 30, 2019, accepted May 31, 2019, date of publication June 5, 2019, date of current version June 20, 2019.

Digital Object Identifier 10.1109/ACCESS.2019.2921088

# X-Band Dual Circularly Polarized Patch Antenna With High Gain for Small Satellites

PAOLO SQUADRITO<sup>ID</sup>, SHUAI ZHANG<sup>ID</sup>, (Senior Member, IEEE),  
AND GERT FRØLUND PEDERSEN<sup>ID</sup>, (Senior Member, IEEE)

Department of Electronic Systems, Antennas, Propagation and Millimeter-Wave Systems Section, Aalborg University, 9220 Aalborg, Denmark

Corresponding author: Shuai Zhang (sz@es.aau.dk)

This work was supported by the InnovationsFonden Project of MARS2.

**ABSTRACT** This paper presents an X-band circularly polarized patch antenna with a simulated high gain of 12.5 dBi and a simulated side-lobe-level of below  $-20$  dB, within the bandwidth of 5.2 %. This single element antenna achieves high gain by exploiting the mode superposition of  $TM_{11} + TM_{13}$  (excited by a circle of vias loading the cavity) and  $TM_{12} + TM_{14}$  (excited by the cavity itself) radiated from the two apertures, respectively. A simple feeding network, consisting of a quadrature hybrid and a couple of  $90^\circ$  bent branches, is used in the design to excite RHCP or LHCP mode in the antenna cavity. A capacitive disk feeding is implemented so that the antenna can be matched to the feeding network, and the super-positioned fields inside the cavity are not disturbed by the feeding pins. This approach makes the design of a dual-sense circularly polarized antenna with high gain easier since the array configuration is not needed. High gain, in combination with a dual-sense circular polarization, makes the proposed antenna particularly attractive for space applications involving small satellites. With the proposed design, it is possible to employ only one antenna rather than two (RHCP and LHCP), thus saving space on the aircraft, which is clearly a limited resource.

**INDEX TERMS** Circular patch, circular polarization, high gain, sidelobes suppression, small satellites.

## I. INTRODUCTION

The access to the space segment is nowadays easier than ever, thanks to the recent advances done in miniaturization technology. As a matter of fact, the number of space mission involving small satellites in their different sizes is exponentially increasing [1]. Despite this recent growth, the concept of small satellite is not new. The relatively low cost of mass production and low launch cost are the main reason why small satellites are so attractive for small private companies or universities. In addition, the flexibility of this approach is another key aspect, which makes possible thanks to modern technologies, different kinds of missions like earth observation, remote sensing and of course communications. Although this comes with several challenges to face. Indeed the limited power on-board and the limited amount of area available are the main critical aspect of this kind of approach to space. The design of the antenna system is essential and different constraints must be taken into account from mission to mission.

The associate editor coordinating the review of this manuscript and approving it for publication was Yang Yang.

For instance in [2], [3], transparent antennas are presented. This particular characteristic allows the allocation of the antenna on top of a solar panel, in order to save space on the platform. An S-band antenna system for earth observation is presented in [4]. This antenna shows a square window which is designed in order to accommodate the imaging system in the center. For downlink communications, deployable monopole or planar patch antennas working in UHF and S-band have been extensively employed, because of their lightweight and low-cost characteristics. For higher bit-rates, X-band is becoming more and more common [5] but, it is well-known that the aforementioned type of antennas in their classical configuration cannot provide the gain needed [6]. Increasing the aperture area of an antenna by employing an array configuration is a commonly used method to increase the gain. Besides the needs of relatively high gain, circularly polarized antennas are preferred since radio waves propagating through the ionosphere are subject to the Faraday Rotation Effect [7]. In [8]–[12] several circularly polarized arrays are presented. Often, both RHCP and LHCP polarizations are desired [13]–[16], which means that in some cases, two different antennas must be employed, so a doubled area is used.

In [13], [14] dual circularly polarized dual band antennas are proposed. With this approach, however, only one polarization per band can be achieved. In [15] an aperture antenna is presented. Dual circular polarization is achieved, in this case, by using a new relatively complex feeding scheme for a four elements array. A low-profile circular patch antenna is presented in [17]. High gain and SLL suppression in a single element are the attractive characteristics of this antenna. On the other hand, this element is linearly polarized so it cannot be employed in several applications.

In this paper, a dual-sense circularly polarized planar antenna is presented. Following the same working principle exploited in [17], a high gain antenna with sidelobe suppression has been designed. Unlike the array configuration just mentioned, the proposed antenna is made by only one element which in turn allows a simple feeding network to be employed. By using a  $90^\circ$  hybrid, indeed, both RHCP and LHCP have been achieved in the same operative band. A capacitive feeding technique, in place of a traditional pin technique, has been employed in the proposed design. It is shown that by doing so, two main advantages are obtained. The first advantage in terms of impedance matching of the antenna to the feeding network. The second advantage in terms of purity of the fields inside the cavity, which are no longer disrupted by the feeding pin. This approach compared with the previously reported CP antennas bring several advantages, particularly for applications involving small satellites. On one hand, employing a single element makes the design of single band dual circularly polarized antennas easier since just a simple feeding network is needed. On the other hand the higher gain (compared with a conventional single element patch antenna) achieved by this design by exploiting the superposition of radiated fields, makes the antenna suitable to be employed in small satellites applications (for instance downlink communications). Thus avoiding dual band antennas like in [13], [14], or relatively complex feeding network like in [15]. This paper is organized as follows. Section II describes the antenna configurations. In this section, the challenges faced to design this kind of antenna and the proposed solution are presented. In section, III measured results and comparison are shown. Conclusion and possible future applications are discussed in section IV.

## II. ANTENNA CONFIGURATION

### A. ANTENNA AND FEEDING NETWORK DESIGN

In Fig.1 the configuration of the proposed antenna is shown. It has a 3 layers structure and the total dimension with regards to the wavelength is  $3.7\lambda$ . The antenna layer is printed on a Roger 4350B with  $\epsilon_r = 3.66$ ,  $\tan \delta = 0.0037$  and thickness  $h_1 = 1.524$  mm. It consist of a single circular element of radius  $R1 = 27$  mm, with a circular slot of width  $g = 0.8$  mm etched at the position  $r_p = 11.03$  mm. A circle of  $N = 20$  grounded vias with non-identical diameter is placed at the position  $r_c = 8.7$  mm. The diameters of the vias are

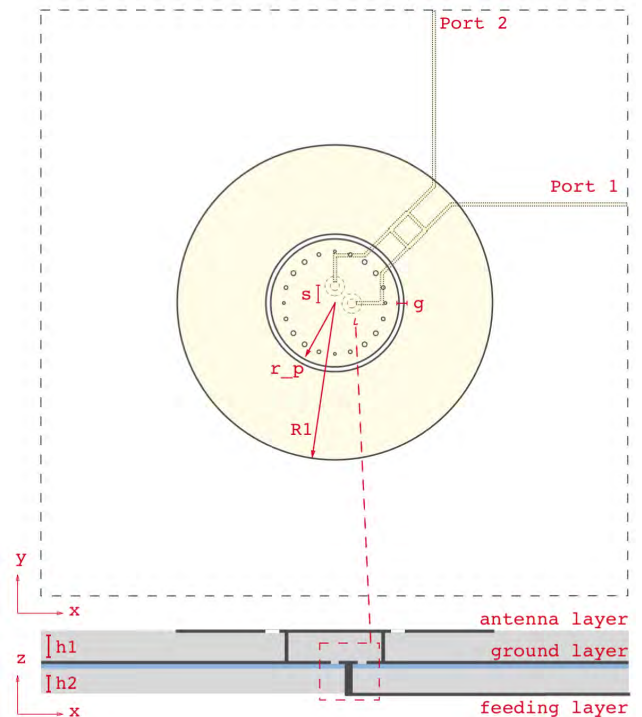


**FIGURE 1.** Top view and side view of the proposed antenna layout. The metallizations are represented in black, the substrates (Roger 4350B) in grey and the glue film (Isola 370HR) in blue. Lines with the same dash step belong to the same layer.

$d_{small} = 0.6$  mm,  $d_{medium} = 0.7$  mm and  $d_{large} = 0.8$  mm. With this choice the symmetry of the antenna in both E-plane and H-plane is preserved, thus allowing better performance in terms of polarization. The ground layer is printed on the other face of the Roger 4350B. Two circular apertures with diameter  $d_1 = 3.4$  mm (Fig.1 and Fig.2a) are etched in the ground plane at position  $s = 3$  mm along the x and y axes. A couple of metallic disks with diameter  $d_2 = 1.6$  mm are then placed in  $s$  and connected to the feeding network through a metallic pin. The feeding layer mainly consists of a quadrature hybrid connected to two  $90^\circ$  bent branches. This layer is printed on a Roger 4003C with  $\epsilon_r = 3.55$ ,  $\tan \delta = 0.0027$  and thickness  $h_2 = 0.2$  mm which in turn is glued to the ground layer through a thin film of Isola 370HR shown in blue in Fig.1.

### B. ANALYSIS OF THE FEEDING TECHNIQUE

A capacitive feeding technique has been chosen for the proposed antenna as shown in Fig.2a. As mentioned before the antenna cavity is fed through a couple of disks printed in the same layer of the ground plane. A common approach, among all, to achieve circular polarization is by exciting two orthogonal components with a  $90^\circ$  phase difference. The two disks are thus orthogonally placed and the  $90^\circ$  phase difference is provided by the quadrature hybrid. It is worthy to point out now that, by the nature of the quadrature hybrid, a dual-sense

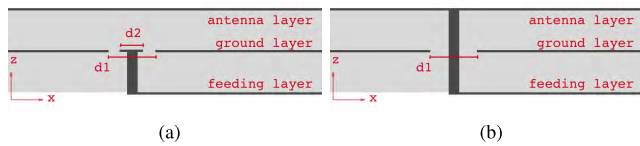


**FIGURE 2.** Side view of the capacitive disk technique (a) made of a disk capacitively coupled with the antenna layer, and the pin technique (b) consisting of a pin going through the ground plane and connecting directly the antenna to the feeding network. For simplicity some details have been removed from this drawings.

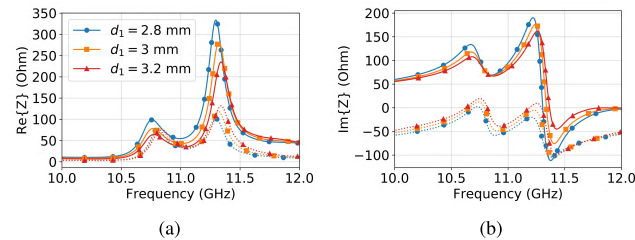


**FIGURE 3.** Simulated real (a) and imaginary (b) parts of the antenna input impedance for pin (solid line) and disk (dotted line) feeding technique.

circularly polarized antenna is obtained. There are two main reasons for choosing a capacitive feeding technique over a traditional feeding with a pin going through a circular aperture in the ground plane and connecting the antenna directly to the feeding network as shown in Fig.2.b. The first reason is related to the input impedance of the antenna. For a patch antenna operating with the fundamental mode, it is well known that the input impedance is maximum at the edge. This is no longer true when high order modes are excited in the cavity. In order to achieve high gain and improved SLL suppression, the proposed antenna exploits a superposition of radiated fields. A superposition of  $TM_{11} + TM_{13}$  (radiating from the circular slot and from the outer aperture respectively) is excited at lower frequency by the circle of vias and a superposition of  $TM_{12} + TM_{14}$  (radiating from the circular slot and from the outer aperture respectively) is excited at higher frequency by the cavity itself. In this case, the input impedance is maximum in a position between the center and the edge, depending on which high order mode is excited [18]. As a consequence of this, it is difficult to match the antenna to the feeding network. Fig.3 shows the real (a) and imaginary (b) part of the input impedance for both the techniques. The pin technique (solid line) shows a higher resistance and reactance compared to the capacitive disk technique (dotted line). Moreover, the two degrees of freedom (the diameter of the circular aperture in the ground plane  $d_1$  and the diameter of the circular disk  $d_2$ ) given by this solution makes the impedance matching of the antenna easier. The second reason is related to the unwanted modes excited in the cavity. In a real scenario, the pin technique excites unwanted modes in the cavity [17]. This effect alters the purity of the  $TM_{1x}$  modes, which as said earlier, are exploited in the proposed design to achieve high gain and sidelobe level

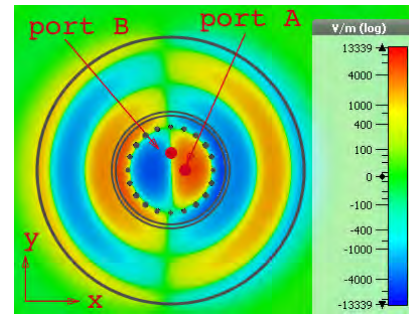


**FIGURE 4.** Z component of the E-field excited in the cavity by only one port at 11 GHz. The edges of the metallic parts are represented in black and the feeding points are represented in red.

suppression. As said before, in applications where circular polarization is needed, a couple of pins are placed inside the cavity in orthogonal position in order to excite two orthogonal polarizations. When a pure  $TM_{1x}$  is excited this additional pin (which excite the orthogonal polarization) lies in a zero-field position. This is shown in Fig.4. The z components of the E-field inside the cavity excited by only port A at 11 GHz is represented. In this situation is clearly shown that port B is placed in a zero-fields area but when unwanted mode are excited this no longer applies. Therefore as a direct consequence, the two pins disrupt each other, narrowing down the radiation performance and deteriorating the isolation between the input port of the antenna. This effect can be mitigated by using a capacitive technique which is intrinsically free of metallic parts inside the antenna’s cavity. It is worth to point out now, for a better understanding of the working principle of this antenna, that since only two modes are excited inside the cavity, only two resonances are shown in Fig.3. Consequently, each mode excited inside the cavity produces a superposition of radiated fields from the two apertures of the antenna.

### III. ANTENNA PERFORMANCE

According to what presented in section II a prototype of the proposed antenna has been realized and measured. The scattering parameters, measured with a Keysight N5227A PNA, are shown in Fig.5. Both simulation and measurement show a wide range where the  $|S_{xx}|$  is below  $-10$  dB, with the exception of Port 1 for the manufactured antenna, which shows a small peak around 11 GHz. Taking into account  $S_{21}$ , the simulated antenna shows an impedance bandwidth of 5.2% from 10.7 GHz to 11.27 GHz highlighted in red in Fig.5. The measured antenna shows an impedance bandwidth of 3.6% from 11 GHz to 11.4 GHz, highlighted in blue in Fig.5. Moreover, compared to the simulated results, the manufactured antenna band appears to be shifted to a slightly higher frequency. This discrepancy is related to a poor manufacture of the antenna which is relatively sensitive to the radius of the vias. This behavior has been observed in [17] already, so the results are not repeated in this work. The anechoic chamber shown in Fig.6 has been used to



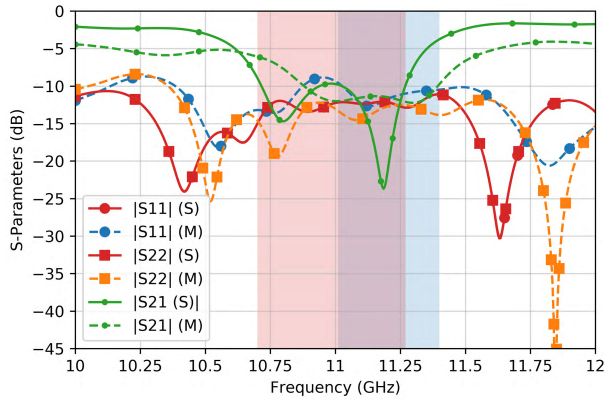


**FIGURE 5.** Measured (M) and Simulated (S)  $|S_{11}|$ ,  $|S_{22}|$  and  $|S_{21}|$ . The impedance bandwidth of the manufactured antenna is highlighted in light blue. Simulated  $|S_{22}|$  is not shown for reasons of symmetry.

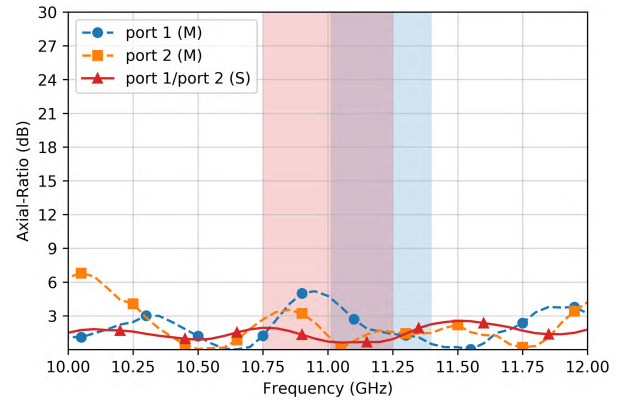


**FIGURE 8.** Measured (M) and Simulated (S) Axial Ratio for port 1 and port 2. The impedance bandwidth of the manufactured antenna is highlighted in light blue.

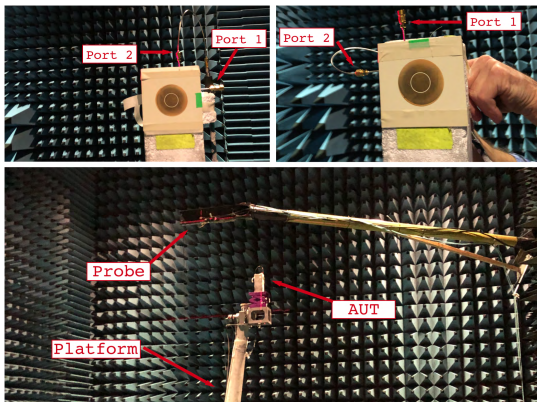


**FIGURE 6.** Measurement setup employed for the proposed antenna. The probe is kept in a fixed position on the arm. The antenna under test is placed on the platform. Rotating the platform the E-plane or H-plane radiation pattern is measured.

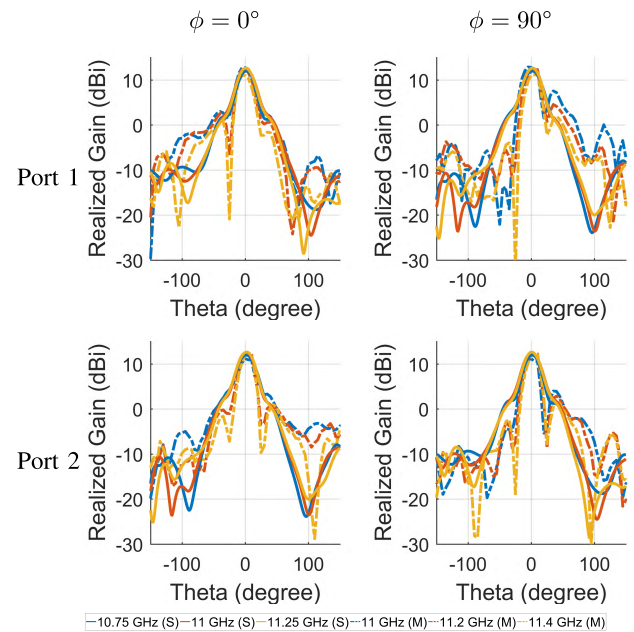


**FIGURE 9.** Measured (M) and Simulated (S) radiation patterns for E-plane and H-plane at three different frequency points. Results are shown for port 1 and port 2.

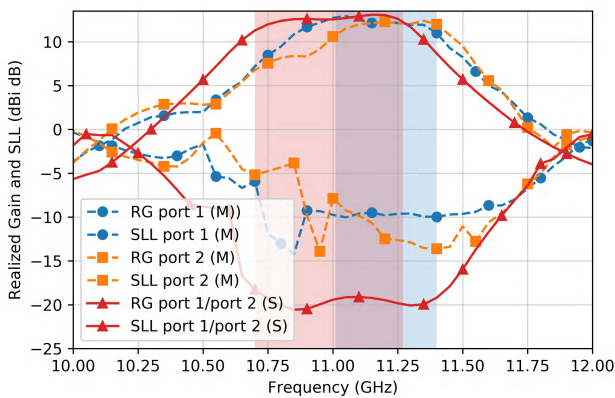


**FIGURE 7.** Measured (M) and Simulated (S) Realized Gain (RG) and Side Lobe Level (SLL) for port 1 and port 2. The impedance bandwidth of the manufactured antenna is highlighted in light blue. For reason of symmetry the simulated results for port 2 are omitted.

measure the radiation performances of the presented antenna. In this setup, the probe is placed on the yellow arm and the AUT is placed on the grey platform. By rotating the platform

a full plane scanning is achieved. In order to measure both E-plane and H-plane, the AUT is thus manually rotated by  $90^\circ$ . Gains and SLL are presented in Fig.7, once again the impedance bandwidth is highlighted in blue. The simulated gain is 13 dBi. The measured gain is around 12.5 dBi, which agrees with the simulated gain, with the only exception of a shift toward slightly higher frequency. On the other hand, simulation and measurement for the SLL seem to be rather different. The simulated SLL is around  $-20$  dB, whereas the measured SLL is around  $-10$  dB. However, the SLL shown by the manufactured antenna is quite similar to the one shown in [17] which is enough for the application. The simulated cross-polarization for both ports shows a cross-pol level around  $-18$  dB at  $\theta = 0^\circ$ , the worst case is around



$\theta = 45^\circ$  where the cross-pol level is 0 dB. Considering the relatively low level of the worst case and the fact that is outside the main beam area, the results are omitted. Results for the axial ratio are presented in Fig. 8. The simulated results show an  $AR < 3$  dB in a large band. The in-band axial ratio level for port 1 is a bit high because of a peak around 11 GHz. On the other hand, measured results for port 2 show better performance with an  $AR < 2$  dB in the whole impedance bandwidth. Due to the symmetry of the structure, the AR for the two ports should be the same thus the differences are due to imperfection in the manufacturing process. Fig. 9 shows the realized gain of the manufactured antenna for both ports in the two main planes compared with the simulated results. The simulated results are shown in the band from 10.75 GHz to 11.25 GHz and the measured results are shown in the band 11 GHz to 11.4 GHz due to the small shift to a higher frequency. The first sidelobe seems to appear around  $\pm 50^\circ$  for the measurement and around  $\pm 110^\circ$  for the simulations, which could explain the difference between the curves in Fig. 7.

#### IV. CONCLUSION

In this paper, an X-band circular polarized patch antenna. Simulations have shown a high gain of 12.5 dBi and a SLL better than  $-20$  dB, in a bandwidth of 5.2 %. For this single element antenna, the high gain has been achieved, by exploiting a superposition of fields radiated from two apertures. A simple feeding network consisting of a quadrature hybrid and a couple of  $90^\circ$  bent branches have been used in the proposed design, in order to excite RHCP or LHCP modes in the antenna cavity. This approach makes the design of a dual sense circularly polarized antenna with high gain easier since the array configuration or other more complex solution are not needed. Because of the advantages in terms of impedance matching and modes purity, a capacitive feeding technique, rather than a pin feeding technique, has been chosen to feed the antenna. High gain, in combination with a dual-sense circular polarization, make the proposed antenna particularly attractive for space applications involving small satellites. For instance, the proposed antenna could be employed for downlink applications where, to the best knowledge of the authors, two separate antennas arrays operating in the same band (one for the RHCP and another one for LHCP) are used. Consequently, space, which is clearly a very limited resource on a small satellite, is saved. It is worth to point out that, for practical reason, a high dielectric constant has been chosen for the manufacturing of this antenna. This choice limits the gain that otherwise would be up to 16 dBi [17] which is considered enough for downlink applications in low earth orbit.

#### REFERENCES

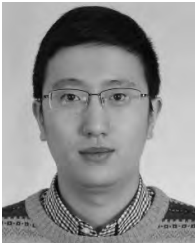
[1] *Nanosatellite Launches Since 1998*. (2018). [Online]. Available: <https://www.nanosats.eu>

- [2] X. Liu, J. Liu, D. R. Jackson, J. Chen, P. W. Fink, and G. Y. Lin, "Broadband transparent circularly-polarized microstrip antennas for cubesats," in *Proc. IEEE Int. Symp. Antennas Propag. (APSURSI)*, Jun./Jul. 2016, pp. 1545–1546.
- [3] J. Sun and K.-M. Luk, "A wideband low cost and optically transparent water patch antenna with omnidirectional conical beam radiation patterns," *IEEE Trans. Antennas Propag.*, vol. 65, no. 9, pp. 4478–4485, Sep. 2017.
- [4] A. Nascetti, E. Pittella, P. Teofilatto, and S. Pisa, "High-gain S-band patch antenna system for earth-observation CubeSat satellites," *IEEE Antennas Wireless Propag. Lett.*, vol. 14, pp. 434–437, Nov. 2015.
- [5] *Nanosatellite Frequencies and Bands*. (2018). [Online]. Available: <https://www.nanosats.eu>
- [6] C. A. Balanis, *Antenna Theory: Analysis and Design*. Hoboken, NJ, USA: Wiley, 2005.
- [7] E. Sorensen, "Magneto-ionic Faraday rotation of the radio signals on 40 MC from satellite 1957  $\alpha$  (Sputnik I)," *IRE Trans. Antennas Propag.*, vol. 9, no. 3, pp. 241–247, May 1961.
- [8] S. Lin and Y. Lin, "A compact sequential-phase feed using uniform transmission lines for circularly polarized sequential-rotation arrays," *IEEE Trans. Antennas Propag.*, vol. 59, no. 7, pp. 2721–2724, Jul. 2011.
- [9] A. Chen, Y. Zhang, Z. Chen, and C. Yang, "Development of a ka-band wideband circularly polarized 64-element microstrip antenna array with double application of the sequential rotation feeding technique," *IEEE Antennas Wireless Propag. Lett.*, vol. 10, pp. 1270–1273, 2011.
- [10] C. J. Deng, Y. Li, Z. J. Zhang, and Z. H. Feng, "A wideband sequential-phase fed circularly polarized patch array," *IEEE Trans. Antennas Propag.*, vol. 62, no. 7, pp. 3890–3893, Jul. 2014.
- [11] S. Mohammadi-Asl, J. Nourinia, C. Ghobadi, and M. Majidzadeh, "Wide-band compact circularly polarized sequentially rotated array antenna with sequential-phase feed network," *IEEE Antennas Wireless Propag. Lett.*, vol. 16, pp. 3176–3179, 2017.
- [12] K. Ding, C. Gao, D. Qu, and Q. Yin, "Compact broadband circularly polarized antenna with parasitic patches," *IEEE Trans. Antennas Propag.*, vol. 65, no. 9, pp. 4854–4857, Sep. 2017.
- [13] J.-D. Zhang, W. Wu, and D.-G. Fang, "Dual-band and dual-circularly polarized shared-aperture array antennas with single-layer substrate," *IEEE Trans. Antennas Propag.*, vol. 64, no. 1, pp. 109–116, Jan. 2016.
- [14] T. Yue, Z. H. Jiang, and D. H. Werner, "A compact metasurface-enabled dual-band dual-circularly polarized antenna loaded with complementary split ring resonators," *IEEE Trans. Antennas Propag.*, vol. 67, no. 2, pp. 794–803, Feb. 2019.
- [15] J. Zhu, S. Liao, Y. Yang, F. Li, and Q. Xue, "60 GHz dual-circularly polarized planar aperture antenna and array," *IEEE Trans. Antennas Propag.*, vol. 66, no. 2, pp. 1014–1019, Feb. 2018.
- [16] Q. Wu, J. Hirokawa, J. Yin, C. Yu, H. Wang, and W. Hong, "Millimeter-wave multibeam endfire dual-circularly polarized antenna array for 5G wireless applications," *IEEE Trans. Antennas Propag.*, vol. 66, no. 9, pp. 4930–4935, Sep. 2018.
- [17] P. Squadrito, S. Zhang, and G. F. Pedersen, "Wideband or dual-band low-profile circular patch antenna with high-gain and sidelobe suppression," *IEEE Trans. Antennas Propag.*, vol. 66, no. 6, pp. 3166–3171, Jun. 2018.
- [18] P. Juyal and L. Shafai, "A novel high-gain printed antenna configuration based on  $TM_{12}$  mode of circular disc," *IEEE Trans. Antennas Propag.*, vol. 64, no. 2, pp. 790–796, Feb. 2016.



**PAOLO SQUADRITO** was born in Catania, Italy, in 1988. He received the B.S. and M.S. degrees in telecommunication engineering from the University of Catania, Catania, in 2013 and 2017, respectively. He is currently pursuing the Ph.D. degree with the Department of Electronic Systems, Aalborg University.

His research interest includes high-gain antenna design for small satellites' applications.



**SHUAI ZHANG** (SM'18) received the B.E. degree from the University of Electronic Science and Technology of China, Chengdu, China, in 2007, and the Ph.D. degree in electromagnetic engineering from the Royal Institute of Technology (KTH), Stockholm, Sweden, in 2013. After his Ph.D. studies, he was a Research Fellow with KTH. In 2010 and 2011, he was a Visiting Researcher with Lund University, Sweden, and Sony Mobile Communications AB, Sweden,

respectively. In 2014, he joined Aalborg University, Denmark, where he is currently an Associate Professor. He was an External Antenna Specialist with Bang & Olufsen, Denmark, from 2016 to 2017. He has coauthored over 60 articles in well-reputed international journals. He holds 16 U.S. or WO patents. His current research interests include mobile terminal mmwave antennas, biological effects, CubeSat antennas, massive MIMO antenna arrays, UWB wind turbine blade deflection sensing, and RFID antennas.



**GERT FRØLUND PEDERSEN** was born in 1965. He received the B.Sc. and E.E. (Hons.) degrees in electrical engineering from the College of Technology in Dublin, Dublin Institute of Technology, Dublin, Ireland, in 1991, and the M.Sc., E.E., and Ph.D. degrees from Aalborg University, Aalborg, Denmark, in 1993 and 2003, respectively. Since 1993, he has been with Aalborg University, where he is currently a Full Professor heading the Antennas, Propagation and Millimeter-Wave Systems

Laboratory with 25 researchers. He is also the Head of the Doctoral School on wireless communication with some 40 Ph.D. students enrolled. He was a Consultant for developments of more than 100 antennas for mobile terminals, including the first internal antenna for mobile phones, in 1994, with lowest SAR, first internal triple-band antenna, in 1998, with low SAR and high TRP and TIS, and, lately, various multiantenna systems rated as the most efficient on the market. He has worked most of the time with joint university and industry projects and have received more than 21\$ million in direct research funding. He is also the Project Leader of the RANGE Project with a total budget of over 8\$ M investigating high-performance centimetre/millimetre-wave antennas for 5G mobile phones. He has been one of the pioneers in establishing over-the-air measurement systems. The measurement technique is now well established for mobile terminals with single antennas. He is also involved in the MIMO OTA measurement. He has published more than 500 peer-reviewed papers, six books, and 12 book chapters. He holds over 50 patents. His research interests include radio communication for mobile terminals especially small antennas, diversity systems, propagation, and biological effects. He has been chairing the various COST groups with liaison to 3GPP and CTIA for over-the-air test of MIMO terminals.

• • •